Supplementary Information

The reagents used, $FeCl_2 \cdot 4H_2O$, $CoCl_2 \cdot 6H_2O$, 2-thiopheneboronic acid, cyclohexanedion-1,2-dioxime (nioxime, H_2Nx), triethylamine, sorbents and solvents were obtained commercially (Acros).

Analytical data (C, H, N content) were obtained with a Carlo Erba model 1106 microanalyzer.

The MALDI-TOF mass spectra were recorded in both the positive and negative spectral regions using a MALDI-TOF-MS Bruker Autoflex mass spectrometer in reflecto-mol mode. The ionization was induced by UV-laser with wavelength 336 nm. The sample was applied to a nickel plate, 2,5-dihydroxybenzoic acid was used as a matrix. The accuracy of measurements was 0.1%.

The IR spectra of the solid samples (KBr tablets) in the range 400 – 4000 cm^{-1} were recorded with a IR200 Thermo Nicolet FT-spectrophotometer.

The UV-vis spectra of the solutions in dichloromethane were recorded in the range 230 – 800 nm with a Lambda 9 Perkin Elmer spectrophotometer. The individual Gaussian components of these spectra were calculated using the SPECTRA program.

The ^{1}H and $^{13}C\{^{1}H\}$ NMR spectra of the complexes obtained were recorded from their CD_2Cl_2 solutions using a Bruker Avance 400 FT-spectrometer.

X-band EPR spectra were acquired on a Bruker Elexsys E580 X/Q-band EPR spectrometer equipped with ER 4118X-MD5W resonator and Oxford Instruments cryogenic system. The glassy samples for the EPR experiments were obtained from 1 mM solutions of the clathrochelate complexes in the toluene:dichloromethane (1:1, v/v) mixture. The EPR spectra were registered using the following parameters: microwave frequency 9.4 GHz, microwave power in the range 0.2 – 0.002 mW, sweep width 1800 G, modulation frequency 100 kHz, modulation amplitude 1 G, conversion time and time constant in the range 20.48 – 81.92 ms, resolution 2048 points.

$CoNx_3(BThioph)_2$. Anal. calc. for $C_{26}H_{30}B_2CoN_6O_6S_2$ (%): C, 46.78; H, 4.50; N, 12.59. Found (%): C, 46.57; H, 4.39; N, 12.43. ^{1}H NMR (CD_2Cl_2): δ (ppm) – 33.7 (br s, 12H, α-CH_2), 5.16 (s, 12H, β-CH_2), 6.20 (br s, 2H, thiophene-3H), 6.57 (s, 2H, thiophene-4H), 6.93 (s, 2H, thiophene-5H). $^{13}C\{^1H\}$ NMR (CD_2Cl_2): δ (ppm) 22.4 (s, β-CH_2), 129.0, 129.9, 132.0 (all s, thiophene). MS (MALDI-TOF): *m/z* (positive range) 667 $[M]^{+\bullet}$; (negative range) – 667 $[M]^{-\bullet}$. IR (cm^{-1}, KBr): 930, 1035, 1061, 1164 ν(N – O), 1225m ν(B – O), 1579 ν(C=N). UV-Vis (CH_2Cl_2): λ_{max} ($\varepsilon \times 10^{-3}$, mol^{-1} L cm^{-1}): 238 (19), 265 (11), 292 (6.4), 360 (4.9), 460 (2.0), 480 (3.1).

$FeNx_3(BThioph)_2$. Anal. calc. for $C_{26}H_{30}B_2FeN_6O_6S_2$ (%): C, 46.78; H, 4.50; N, 12.59. Found (%): C, 46.66; H, 4.36; N, 12.39. MS (MALDI-TOF): *m/z* (positive range) 664 $[M]^{+\bullet}$; (negative range) – 664 $[M]^{-\bullet}$. ^{1}H NMR (CD_2Cl_2): δ (ppm) 1.68 (s, 12H, β-CH_2), 2.79 (s, 12H, α-CH_2), 7.00 (m, 2H, thiophene-3H), 7.18 (m, 2H, thiophene-4H), 7.30 (m, 2H, thiophene-5H). $^{13}C\{^1H\}$ NMR (CD_2Cl_2): δ (ppm) 23.5 (s, β-CH_2), 28.2 (s, α-CH_2), 128.8, 129.2, 131.9 (all s, thiophene), 154.2 (s, C=N). IR (cm^{-1}, KBr): 932, 1033, 1058, 1163 ν(N – O), 1224m ν(B – O), 1582 ν(C=N). UV-Vis (CH_2Cl_2): λ_{max} ($\varepsilon \times 10^{-3}$, mol^{-1} L cm^{-1}): 233 (23), 252 (11), 283 (5.7), 297 (4.4), 348 (1.9), 441 (6.5), 452 (11).

Cyclic voltammetry (CV) experiments were carried out in acetonitrile solutions with 0.1M ((*n*-$C_4H_9)_4N)BF_4$ as a supporting electrolyte using a model Parstat 2273 (Prinston Applied Research, USA) potentiostat with a conventional one-compartment three-electrode cell (10 ml of solution). Glass carbon (GC) electrode with an active surface area of 0.125 cm^2 was used as a working electrode. The electrode was thoroughly polished and rinsed before measurements. A platinum counter electrode and a standard $Ag/AgCl/KCl_{aq}$. reference electrode were applied. The measurements were performed at scan rates from 50 to 2000 mV s^{-1}. All the solutions were thoroughly deaerated by passing argon through them before the CV experiments and above them during the measurements.

Controlled-potential electrolysis. 25 mM $HClO_4$ acetonitrile solution with 0.1 M $((n\text{-}C_4H_9)_4N)BF_4$ as a supporting electrolyte was electrolyzed for 60 min in the presence of the complexes $CoNx_3(BThioph)_2$ and $FeNx_3(BThioph)_2$ (c = 1 mM) at – 700 and – 1350 mV, respectively. 50 mM $((C_2H_5)_3N)Cl$ acetonitrile solution with 0.1 M $((n\text{-}C_4H_9)_4N)BF_4$ as a supporting electrolyte was electrolyzed for 60 min in the presence of the complexes $CoNx_3(BThioph)_2$ and $FeNx_3(BThioph)_2$ (c = 1 mM) at – 700 and – 1350 mV, respectively. The production of the molecular hydrogen was confirmed by gas chromatography analysis.

Hydrogen Detection. Gas chromatography analysis of gases evolved during the electrolysis was performed with a Varian 450 GC equipped with a pulsed discharge helium ionization detector D-4-I-VA38-R. Hydrogen production was quantitatively detected using a 30 m-in-length stainless steel column with inside diameter 250 μm at 120°C for the detector and at 80°C for the oven. The carrier gas was helium flowing at a rate of 40 ml min^{-1}. The injections (250 μL) were performed *via* a sampling loop. The retention time of gaseous H_2 was 2.48 min.

Kinetic studies. To estimate the k_{obs} values for the electrocatalytic process $2H^+/H_2$, we used an eq. 1 for the pseudo first-order reaction [S1 – S4]:

$$\frac{i_c}{i_p} = \frac{n}{0.4463}\sqrt{\frac{RTk_{obs}}{F\nu}} \qquad (1),$$

where i_c is the catalytic plateau current, i_p is the noncatalytic peak current (here taken from the reversible reduction peak assigned to the $Co^{2+/+}$ or $Fe^{2+/+}$ redox couple in acetonitrile), T = 298.15 K, F is Faraday constant, and υ is a scan rate.

To obtain the values of k_{obs}, we used the method developed in [S5]. A detailed study of a dependence of the catalytic current for the acetonitrile solutions of the complexes $CoNx_3(BThioph)_2$ and $FeNx_3(BThioph)_2$ *vs* scan rate was performed. A catalytic current is independent on scan rates exceed 1000 mV s^{-1} (Figs. SI3 – SI6). If we assume that two electrons are passed for each H_2 molecule produced (n = 2), and an acid concentration does not change significantly in the course of an

experiment, the eq. 2 can be transformed into the eq. 3 allowing to calculate the catalytic turnover frequency k_{obs}.

$$\frac{i_{cat}}{i_p} = \frac{n}{0.4463}\sqrt{\frac{RT\left(k[H^+]\right)}{F\upsilon}} \qquad (2)$$

$$k_{obs} = \upsilon \cdot \left(\frac{i_{cat}/i_p}{0.72}\right)^2 \qquad (3)$$

X-ray crystallography. The details of crystal data collection and refinement for the complexes $CoNx_3(BThioph)_2 \cdot CHCl_3$ and $FeNx_3(BThioph)_2 \cdot CH_2Cl_2$ complexes are listed in Table S1. Single-crystal X-ray diffraction experiments were carried out at 100(2) K with a Bruker Apex II CCD area detector (graphite monochromated Mo-Kα radiation for the cobalt clathrochelate and Cu-Kα radiation with microfocus tube with multilayer optics for the iron macrobicycle). Reflections intensities were corrected by a semi-empirical method using SADABS program [S6]. The structures were solved by the direct method and refined by full-matrix least squares against F^2 on all data using SHELXTL software [S7]. Nonhydrogen atoms were refined in anisotropic approximation except the disordered ones in the clathrochelate molecules of 2-thiopheneboron-capped macrobicycle, one of the two apical substituents is disordered (with the site occupancies equal to 0.7 : 0.3 and 0.8 : 0.2, respectively); both of these disordered 2-thiophene substituents are situated in the same plane. Positions of the hydrogen atoms were calculated and refined using the riding model with isotropic temperature factors $U_{iso} = 1.2U_{eq}(C)$, where U_{eq} values are the equivalent isotropic parameters of parent atoms.

Supporting Information References

[S1] C.P. Andrieux, J.M. Dumas-Bouchiat, J.M. Saveant, *J. Electroanal. Chem*. 1980, 113, 1−18.

[S2] J.M. Saveant, E. Vianello, *Electrochim. Acta* 1965, 10, 905−920.

[S3] J.M. Saveant, E. Vianello, *Electrochim. Acta* 1967, 12, 629− 646.

[S4] J.M. Saveant, *Chem. Rev*. 2008, 108, 2348−2378.

[S5] M.L. Helm, M.P. Stewart, R.M. Bullock, M.R. DuBois, D.L. DuBois, *Science* 2011, 333, 863−866.

[S6] G.M. Sheldrick (1998). SADABS v.2.01, Bruker/Siemens Area Detector Absorption Correction Program, Bruker AXS, Madison, Wisconsin, USA.

[S7] G.M. Sheldrick, *Acta Cryst.* A64 (2008) 112.

[S8] Y.Z. Voloshin, A.Y. Lebedev, V.V.Novikov, A.V. Dolganov, A.V. Vologzhanina, E.G. Lebed, A.A. Pavlov, Z.A. Starikova, M.I. Buzin, Y.N.Bubnov, *Inorg. Chim. Acta*, 2012, submitted, ICA-D-12-00696.

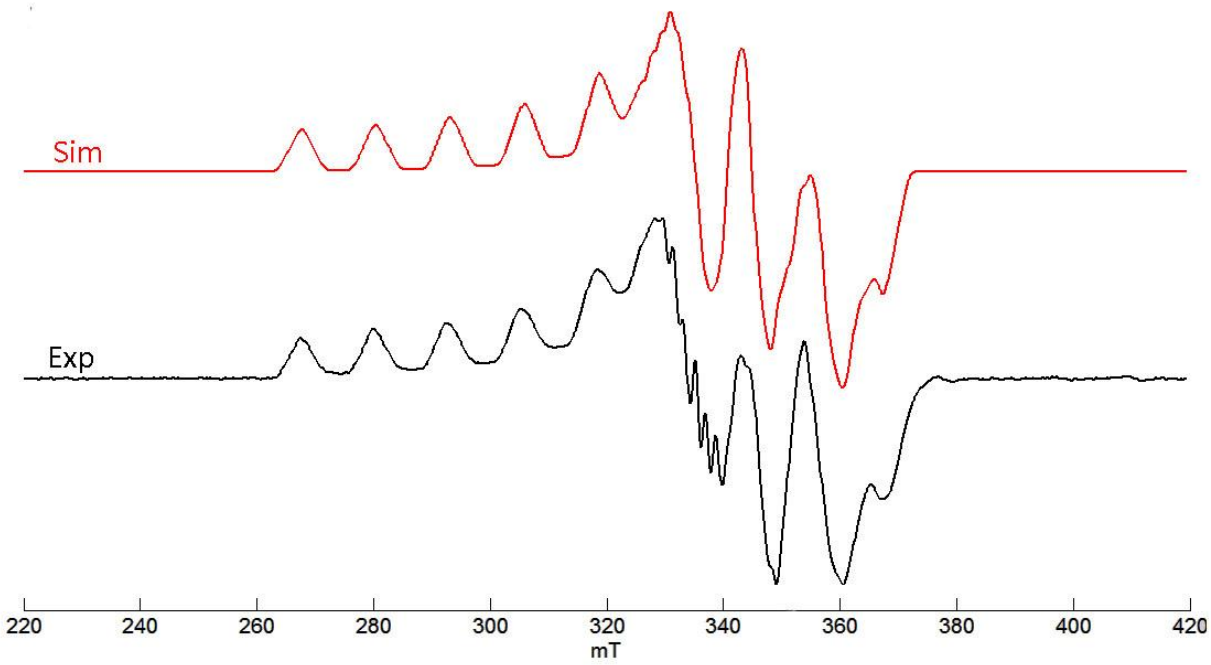

Fig. S1. The experimental and simulated EPR spectra of the clathrochelate $CoNx_3(BThioph)_2$ at 30K. The simulation parameters are as follows: g_{xx} = 1.950, g_{yy} = 2.090, g_{zz} = 2.215, A_{xx} = 50, A_{yy} = 23, A_{zz} = 395 MHz.

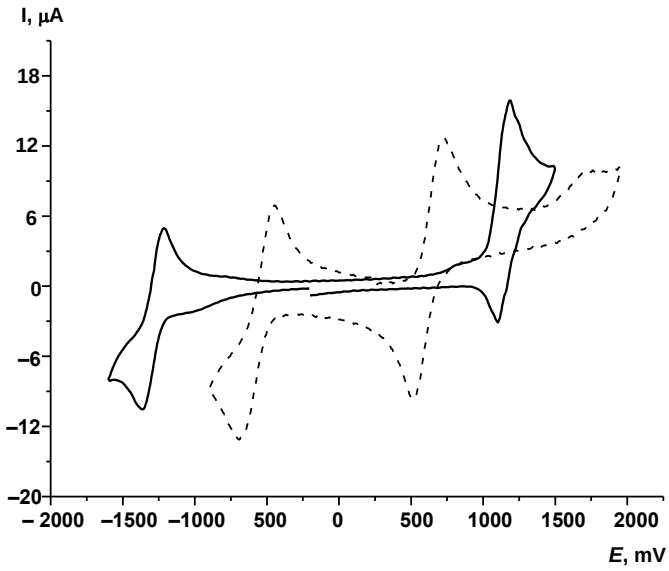

Fig. S2. CV for 3 mM acetonitrile solution of the clathrochelates $FeNx_3(BTioph)_2$ (solid line) and $CoNx_3(BTioph)_2$ (dashed line) at scan rate 200 mV s^{-1} on GC electrode.

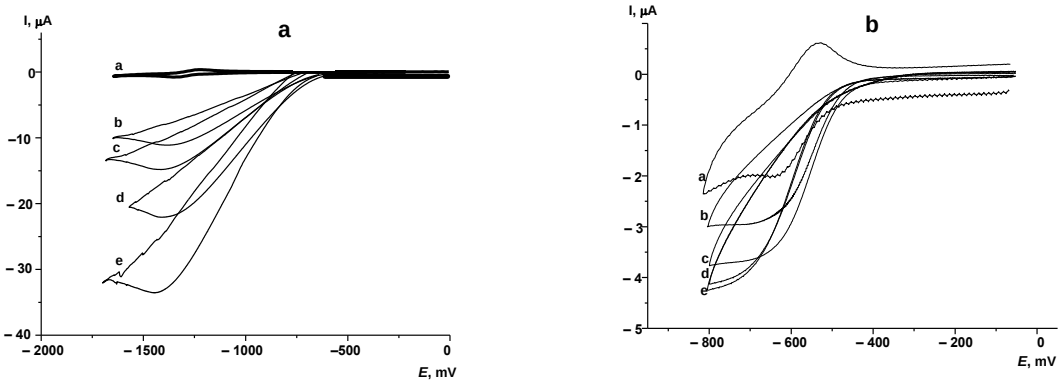

Fig. S3. CVs of the clathrochelates $FeNx_3(BTioph)_2$ (**a**) and $CoNx_3(BTioph)_2$ (**b**) (c = 1 mM) on GC electrode in 0.1 M $((n\text{-}C_4H_9)_4N)BF_4$ acetonitrile solution in the absence (a) and in the presence of $((C_2H_5)_3NH)Cl$: 5 (b), 10 (c), 15 (d), and 25 mM (e) at scan rate 100 mV s^{-1}.

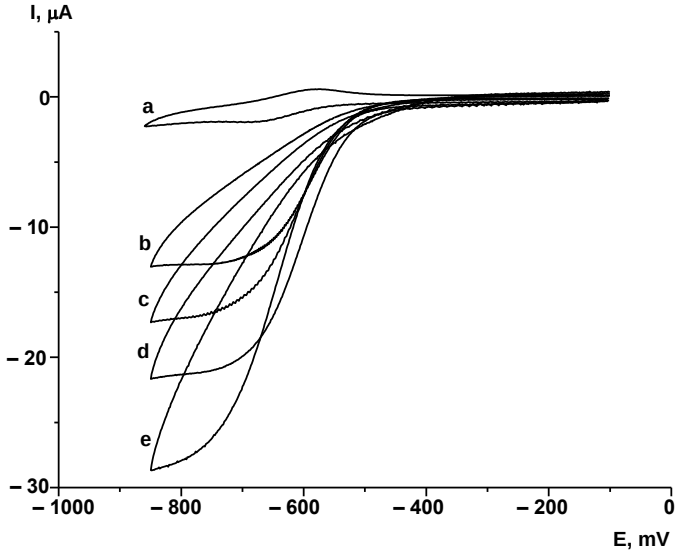

Fig. S4. CVs of 1 mM clathrochelate $CoNx_3(BTioph)_2$ on GC electrode in 0.1M $((n\text{-}C_4H_9)_4N)BF_4$ acetonitrile solution in the absence (**a**) and in the presence of $HClO_4$: 5 (**b**), 10 (**c**), 15 (**d**), and 25 mM (**e**) at scan rate 100 mV s^{-1}.

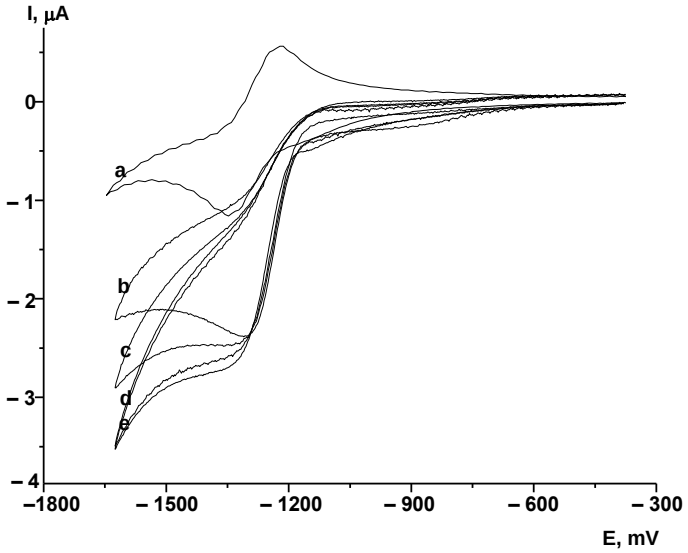

Fig. S5. CVs of 1 mM clathrochelate $FeNx_3(BTioph)_2$ on GC electrode in 0.1 M $((n\text{-}C_4H_9)_4N)BF_4$ acetonitrile solution in the absence (**a**) and in the presence of $HClO_4$: 5 (**b**), 10 (**c**), 15 (**d**), and 25 mM (**e**) at scan rate 100 mV s^{-1}.

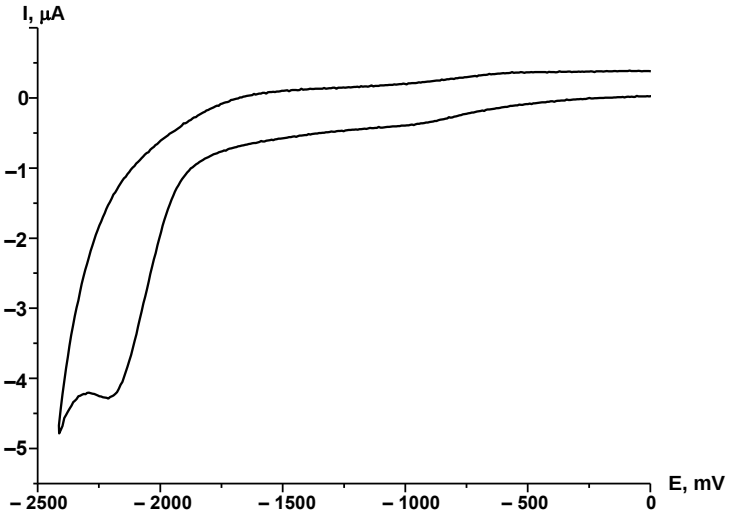

Fig. S6 CV for 1 mM acetonitrile solution of the $(Et_3NH)Cl$ at scan rate 200 mV s^{-1} on GC.

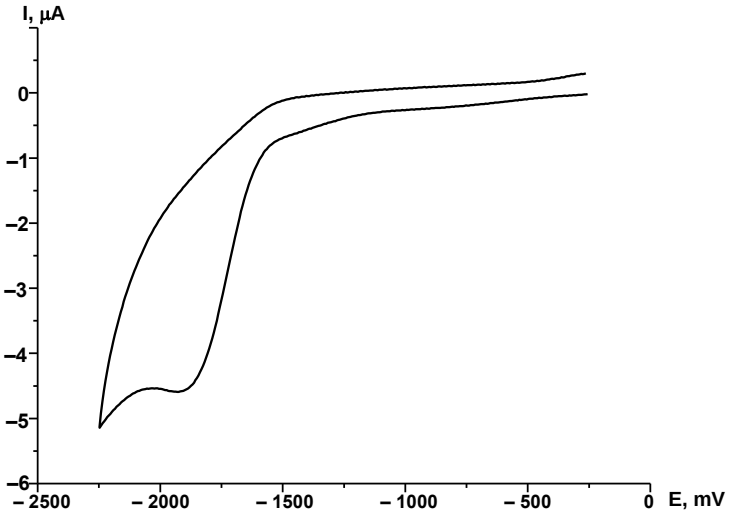

Fig. S7. CV for 1 mM acetonitrile solution of the $HClO_4$ at scan rate 200 mV s^{-1} on GC.

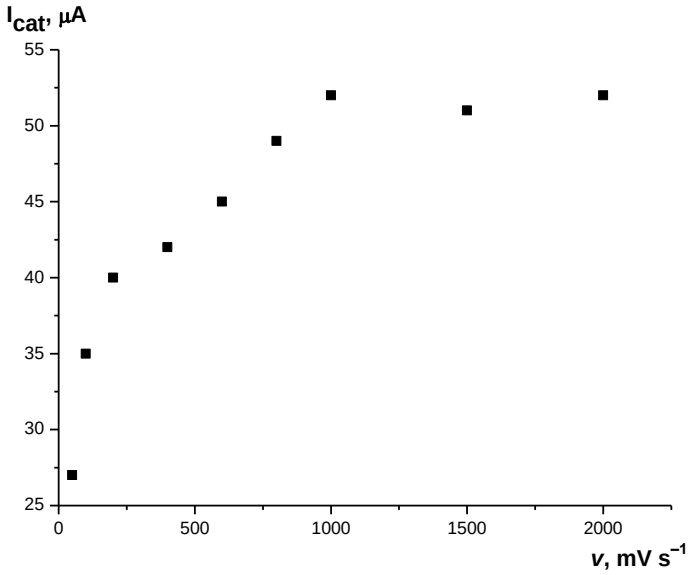

Fig. S8. Plot of I_{cat} *vs* scan rate for 1 mM acetonitrile solution of the complex $FeNx_3(BTioph)_2$ in the presence of 25 mM $((C_2H_5)_3NH)Cl$.

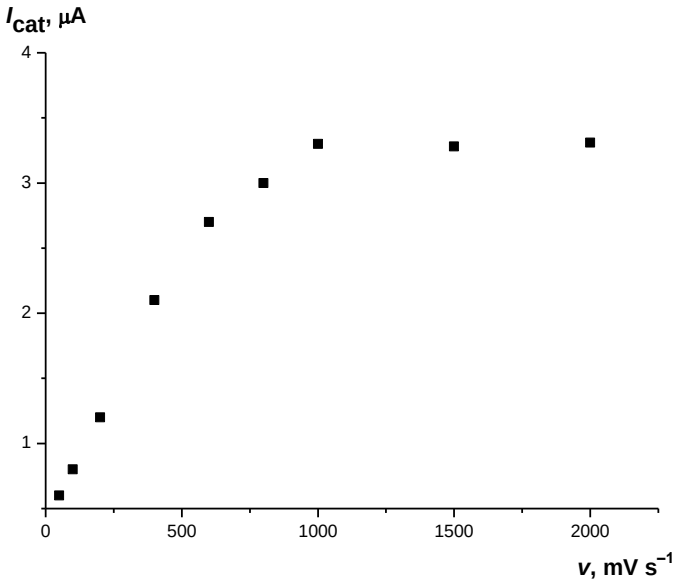

Fig. S9. Plot of I_{cat} *vs* scan rate for 1 mM acetonitrile solution of the complex $FeNx_3(BTioph)_2$ in the presence of 25 mM $((C_2H_5)_3NH)Cl$.

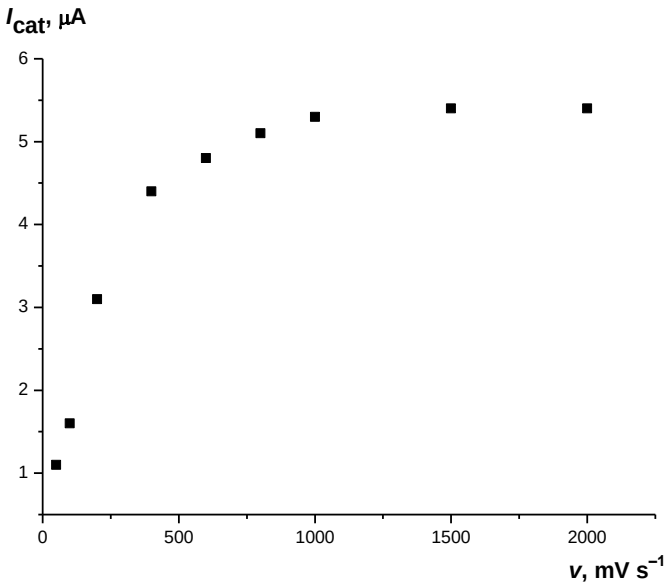

Fig. S10. Plot of I_{cat} *vs* scan rate for 1 mM acetonitrile solution of the complex $FeNx_3(BTioph)_2$ in the presence of 25 mM $HClO_4$.

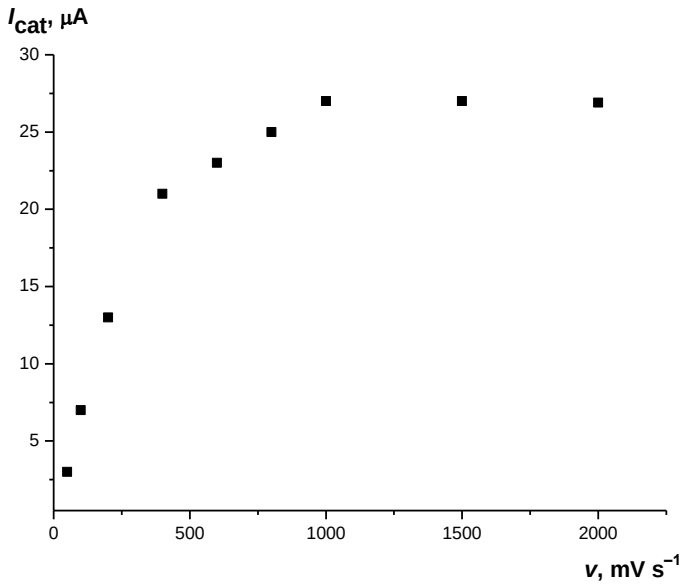

Fig. S11. Plot of I_{cat} *vs* scan rate for the 1 mM acetonitrile solution of the complex $CoNx_3(BTioph)_2$ in the presence of 25 mM $HClO_4$.

Table S1. Crystallographic data and refinement parameters for the 2-thiopheneboron-capped cobalt and iron(II) tris-nioximates

	$CoNx_3(BThioph)_2 \cdot CHCl_3$	$FeNx_3(BThioph)_2 \cdot CH_2Cl_2$
Empirical formula	$C_{26}H_{30}B_2FeN_6O_6S_2 \cdot CHCl_3$	$C_{26}H_{30}B_2FeN_6O_6S_2 \cdot CH_2Cl_2$
Fw	786.60	749.08
Color, habit	dark-brown, plate	dark-orange, prism
Crystal size (mm^3)	0.43 × 0.26 × 0.07	0.16 × 0.15 × 0.09
a (Å)	11.1528 (8)	11.6442 (2)
b (Å)	18.4231 (14)	11.9248 (2)
c (Å)	15.9011 (13)	13.3359 (2)
α (°)	90	92.188 (1)
β (°)	91.971 (2)	104.060 (1)
γ (°)	90	115.847 (1)
V ($Å^3$)	3265.3 (4)	1594.41 (5)
Z	4	2
Crystal system	monoclinic	triclinic
Space group	$P2_1/c$	$P\overline{1}$
d_{calc} ($g \cdot cm^{-3}$)	1.600	1.560
μ (mm^{-1})	0.951	7.001
Min. / max. transmission coeff.	0.745, 0.936	0.376, 0.530
2θ max (°)	56	128
Independent reflections (R_{int})	7887 (0.066)	5148 (0.033)
Obs.refl./restraints/ parameters	5580 / 6 / 416	4886 / 20 / 427
R,[a] % [$F^2 > 2\sigma(F^2)$]	0.044	0.029
R_w,[b] % (F^2)	0.093	0.086
GOF[c]	1.01	1.00
Largest diff. peak and hole (e $Å^{-3}$)	1.57 and – 0.86	0.41 and – 0.57
F(000)	1612	772

Table S2. The main geometrical parameters of the macrobicyclic cobalt and iron(II) tris-nioximates

Parameter	$CoNx_3(BThioph)_2$	$CoNx_3(Bn\text{-}C_4H_9)_2$ [S8]	$FeNx_3(BThioph)_2$	$FeNx_3(Bn\text{-}C_4H_9)_2$ [S8]
Co – N (Å)	1.885(2) – 2.115 (2)	1.876(4) – 2.063(4)	1.904(2) – 1.920(2)	1.898 – 1.913
av. Co – N (Å)	1.970	1.943	1.912	1.906
Δ (Å)	0.23	0.19	0.02	0.02
B – O (Å)	1.492(3) – 1.507(3) *av.* 1.498	1.502	1.484(3) – 1.503(3) *av.* 1.493	1.499
N – O (Å)	1.367(2) – 1.382(2) *av.* 1.375	1.330	1.371(2) – 1.380(2) *av.* 1.378	1.371
C=N (Å)	1.283(3) – 1.303(3) *av.* 1.297	1.295	1.301(3) – 1.309(3) *av.* 1.305	1.302
C – C (Å)	1.444(3) – 1.479(3) *av.* 1.458	1.412	1.434(3) – 1.443(3) *av.* 1.439	1.434
B – C (Å)	1.581(4) – 1.585(4) *av.* 1.583	1.545	1.582(3) – 1.588(3) *av.* 1.586	1.587
φ (°)	4.3	7.0	18.6	20.3
α (°)	38.5	37.5	39.1	39.1
h (Å)	2.45	2.36	2.36	2.36